RESULTS AND PROSPECTS FROM THE SUDBURY NEUTRINO OBSERVATORY

Scott Oser
Department of Physics & Astronomy
University of British Columbia, Vancouver, BC V6T 1Z1, Canada, and
University of Pennsylvania, Philadelphia, PA 19104

Representing the SNO Collaboration

ABSTRACT

The Sudbury Neutrino Observatory (SNO) is a water Cherenkov detector for solar neutrinos that uses 1 kton of pure heavy water (D_2O) as its target material. By observing charged current and neutral current interactions of ^{8}B solar neutrinos on deuterium, SNO has established that a substantial fraction of the solar ^{8}B flux converts from ν_e to other active neutrino flavors, resolving the so-called "solar neutrino problem". Results from SNO and other solar neutrino experiments strongly favor the "Large Mixing Angle" solution to the solar neutrino problem. Dissolving sodium chloride into the heavy water provides enhanced sensitivity to neutral current interactions, and permits a measurement of the total active ^{8}B solar neutrino flux without any assumptions about the energy dependence of the observed flavor oscillation. In addition to studying solar neutrino oscillations, SNO also has unique sensitivity to solar antineutrinos through $\bar{\nu}_e$ charged current interactions on deuterons. I will review the most recent results from the SNO experiment, including first results from the salt phase that were released after the 2003 SLAC Summer Institute.

1 Introduction to solar neutrinos

1.1 Neutrino production in the Sun

The Sun is an intense source of neutrinos with energies in the $\sim$ MeV range. These neutrinos are produced by the nuclear fusion reactions that power the Sun:

$$4p + 2e^- \rightarrow^4 \mathrm{He} + 2\nu_e + 26.731 \text{ MeV} \quad (1)$$

Nuclear fuel burning proceeds via a chain of individual reactions, known as the *pp* chain, as shown in Figure 1. Three reactions in this chain (*pp*, ^{7}Be, and ^{8}B) produce neutrinos with experimentally accessible energies in significant numbers. The shapes of the neutrino energy spectra produced by these reactions, shown in Figure 2, depend only on the kinematics and nuclear physics of the reactions, and not on astrophysical conditions inside the Sun. In fact, the spectral shapes can be measured terrestrially in most cases. The rates of each reaction, and the resulting neutrino fluxes, do depend on the astrophysics, however. Detailed astrophysical calculations, often referred to as "standard solar models" (SSM), predict the rates of each reaction.[1]

1.2 Experimental results prior to SNO

Solar neutrino experiments detect neutrinos through either "radiochemical" or "real time" techniques. The first solar neutrino experiment was Ray Davis' chlorine radiochemical experiment.[2] This experiment looked for neutrino-induced transmutation of chlorine through the reaction $^{37}\mathrm{Cl} + \nu_e \rightarrow e^- +^{37}$ Ar. The energy threshold of this reaction is 0.8 MeV, making the experiment primarily sensitive to ^{7}Be and ^{8}B neutrinos (see Figure 2). By measuring the rate of argon production in a large tank of perchloroethylene, Davis inferred a solar neutrino flux that was just 1/3 of the SSM prediction. This large disagreement with theoretical prediction was the first sign of what became known as the "solar neutrino problem". Davis was awarded a share of the 2002 Nobel Prize in Physics for this pioneering work.

The surprising results of the chlorine experiment prompted other researchers to develop further experiments. The SAGE and GNO/GALLEX radiochemical experiments looked at ν_e interactions on gallium with the reaction $^{71}\mathrm{Ga} + \nu_e \rightarrow e^- +^{71}$ Ge. This reaction has a very low energy threshold of 0.23 MeV, making it

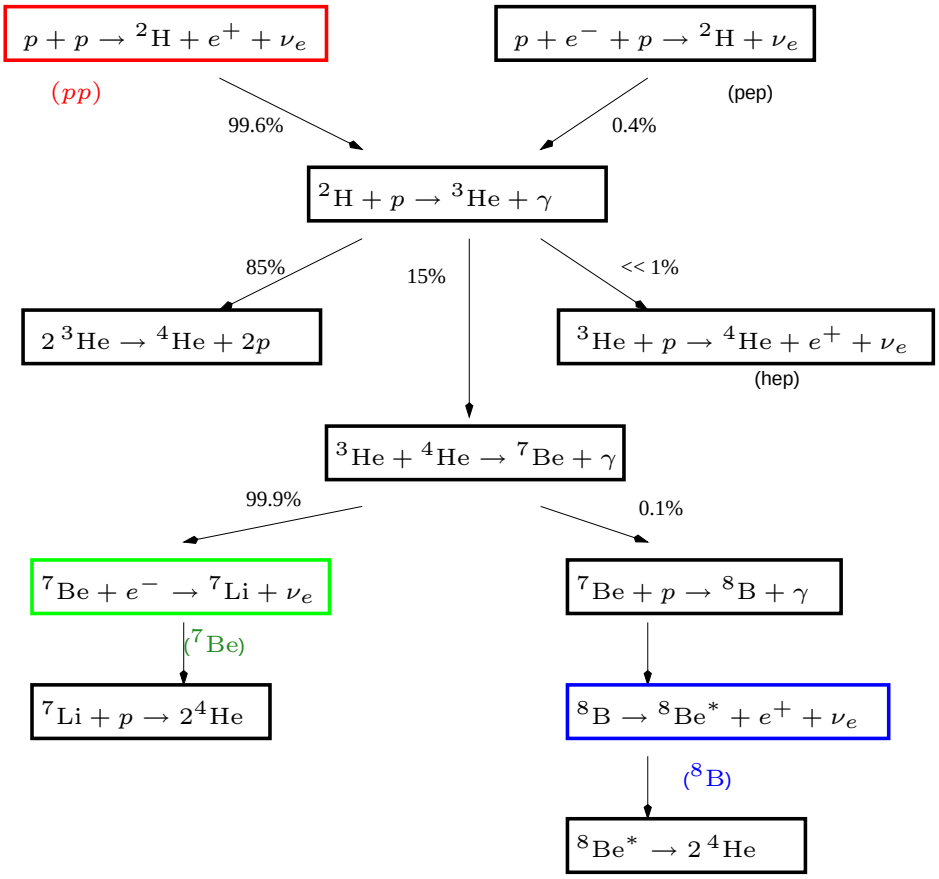

Figure 1: The *pp* reaction chain. The *pp*, ^{7}Be, and ^{8}B reactions produce neutrinos at experimentally accessible energies.

0-0

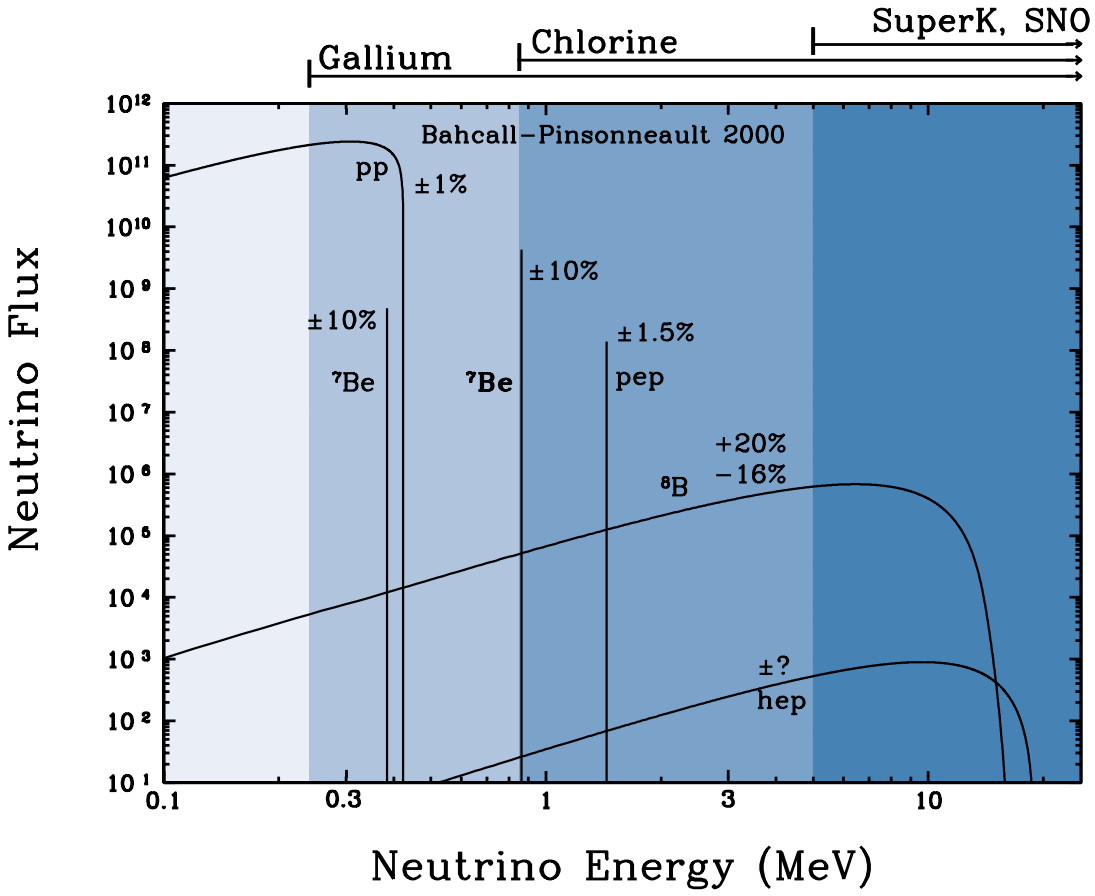

Figure 2: Neutrino energy spectra produced by reactions in the *pp* fusion chain. Figure courtesy of John Bahcall.

sensitive to the predominant *pp* neutrino flux. The gallium experiments confirmed the deficit of observed neutrinos relative to the theoretical prediction, measuring a rate that is ~ 0.55 times the SSM expectation.[3–7]

A different experimental approach is to detect neutrinos in real time by observing elastic scattering of atomic electrons by neutrinos. This technique has been used successfully by the Kamiokande and Super-Kamiokande experiments. This method observes the relativistic electron produced by $\nu + e^- \rightarrow \nu + e^-$ reactions in water. If the scattered electron has sufficient energy, it will emit Cherenkov radiation in a cone that can be detected by arrays of photomultiplier tubes. This "water Cherenkov" technique has many advantages: the electrons are scattered away from the Sun, demonstrating their solar origin; the energy of the scattered electron can be measured, giving a rough idea of the neutrino's energy; and the arrival time of each neutrino is recorded, allowing studies of short- and long-term time variations in the interaction rate. Unlike the radiochemical experiments, the water Cherenkov method is not exclusively sensitive to ν_e's, since ν_μ and ν_τ also elastically scatter electrons, albeit with a cross section that is six times smaller than that for ν_e's. The detection threshold for elastic scattering is around 5 MeV, making these experiments sensitive only to ν's from the ^{8}B branch. The latest results from the Super-Kamkiokande experiment measure an elastic scattering rate that is ~ 0.47 of the SSM prediction, again showing a large disagreement between the measured and theoretical fluxes.[8,9] In 2002 Masatoshi Koshiba was awarded a share of the Nobel Prize in Physics for his work to develop the water Cherenkov technique.

Figure 3 shows the ratio of the measured rate to the SSM prediction for each type of experiment, plotted as a function of the energy threshold for each measurement. All experiments see a deficit of neutrinos relative to SSM prediction, and the size of the deficit depends on the energy.

1.3 Neutrino oscillations

While all experiments have shown a ν flux deficit relative to SSM predictions, interpretation of the results is complicated by the fact that the three classes of experiments, with three different energy thresholds, are sensitive to different neutrino-producing reactions in the Sun. The energy dependence of the deficit, and the relatively small uncertainties in the theoretical predictions, suggested that

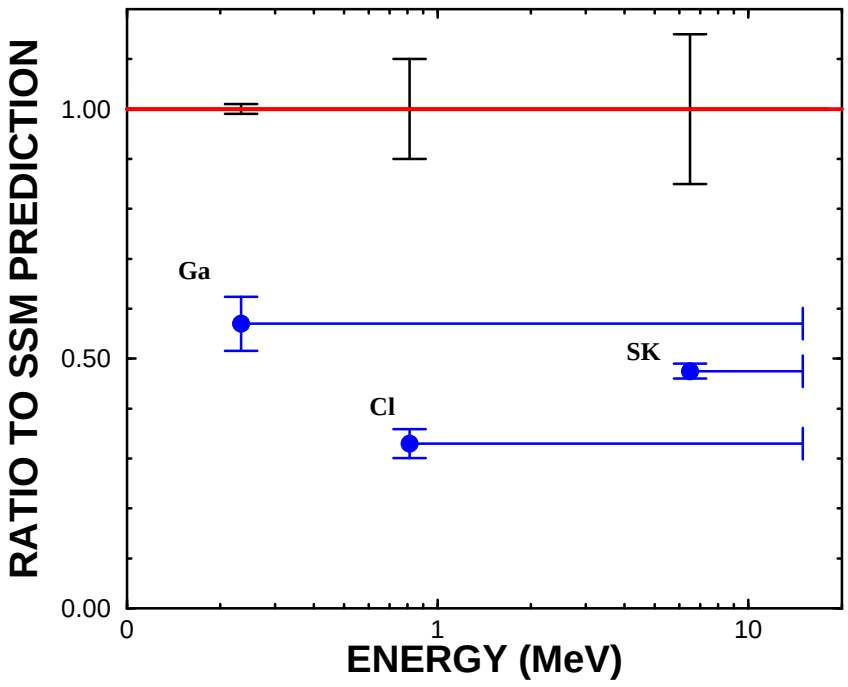

Figure 3: Measured neutrino fluxes from different classes of solar neutrino experiments prior to SNO. The x-axis shows the energy threshold of each experiment, while the y-axis shows the ratio of the measured neutrino rate to the SSM prediction. The error bars on the red line at 1.0 illustrate the size of the theoretical uncertainty.

new neutrino properties might be needed to reconcile the experiment results with the astrophysical predictions. By far the simplest such extension is the possibility of neutrino flavor oscillation.

Neutrino oscillation models posit that neutrino flavor eigenstates $(\nu_e, \nu_\mu, \nu_\tau)$ are not identical to neutrino mass eigenstates, but exhibit mixing similar to the flavor mixing seen for quarks between weak and strong eigenstates.[10] For the simple case of two-flavor mixing, we can write:

$$\begin{aligned} |\nu_e\rangle &= \cos\theta\ |\nu_1\rangle + \sin\theta\ |\nu_2\rangle \\ |\nu_\mu\rangle &= -\sin\theta\ |\nu_1\rangle + \cos\theta\ |\nu_2\rangle \end{aligned}$$

If the mass eigenstates ν_1 and ν_2 have different masses, then in vacuum ν_1 and ν_2 will propagate with different time dependencies, and can develop a non-zero relative phase. As a result, if at $t = 0$ the neutrino is initially in a pure ν_e state $(|\nu(t=0)\rangle = |\nu_e\rangle)$, then at some later time it may contain some admixture of ν_μ, so that $|\langle\nu_\mu|\nu(t)\rangle|^2 > 0$. What was originally purely an electron neutrino could then have some probability to interact as a ν_μ.

Neutrino oscillations provide a neat solution to the problem of the missing solar neutrinos. The original solar neutrino experiments were sensitive almost exclusively to ν_e's. If a substantial fraction of the solar neutrinos had oscillated to non-electron flavors, they would not interact in the detectors, and would appear to be "missing". Neutrino oscillation provides a simple way to reconcile the theoretical SSM neutrino flux predictions with observations. It is not too hard to show that the oscillation probability of neutrinos propagating in vacuum depends on the mixing angle θ and on the difference in the squares of the neutrino masses $(\Delta m^2 \equiv m_2^2 - m_1^2)$ by:

$$P(\nu_e \to \nu_\mu) = \sin^2 2\theta \sin^2\left[1.27\left(\frac{\Delta m^2}{1\ \mathrm{eV}^2}\right)\left(\frac{L}{1\ \mathrm{km}}\right)\left(\frac{1\ \mathrm{MeV}}{E}\right)\right] \qquad (2)$$

Here, L is the distance through which the neutrino has travelled and E is its energy.

Matter effects inside the Sun can significantly alter the oscillation probabilities.[10] Because ν_μ's and ν_τ's at solar neutrino energies interact with electrons inside the Sun only by neutral current processes (Z boson exchange), while ν_e's also have charged current diagrams (W boson exchange), there is a difference in the effective Hamiltonian of electron neutrinos travelling through matter compared to other neutrino flavors. This means that an electron neutrino produced

inside the Sun will have a different effective decomposition into mass eigenstates than will a ν_e in vacuum. The result is that ν_e's produced in the Sun can undergo resonant conversion to other flavors over a wide range of mixing parameters. For some values of the mixing parameters, matter effects can also produce further neutrino oscillations for neutrinos travelling through the Earth. This can result in a "day-night asymmetry", since neutrinos reaching a detector at night must pass through a long pathlength of matter in the Earth that neutrinos coming during daytime do not encounter. The result can be a variation in the neutrino flavor content with the pathlength of matter the neutrinos pass through.

While neutrino oscillations provide a simple solution to the solar neutrino problem, one major experimental caveat remains. All of the evidence for solar neutrino oscillation up to the release of first results from the Sudbury Neutrino Observatory consisted of deficits of observed neutrino fluxes compared to complicated SSM predictions. It is perhaps dangerous to believe in physics beyond the Standard Model on the sole basis of a *failure* to observe the full expected flux. *Direct* evidence for neutrino oscillation, such as observation of non-electron flavors, distortions in the neutrino energy spectra, or a day-night asymmetry, until very recently was utterly lacking.

2 Results from SNO's D_2O phase

The Sudbury Neutrino Observatory (SNO) is a water Cherenkov detector for solar neutrinos located 2 km underground in the Creighton nickel mine near Sudbury, Ontario.[11] Like previous water Cherenkov detectors, SNO detects Cherenkov light from relativistic electrons produced by neutrino interactions in water. Unlike previous detectors, the central volume of SNO is not filled with regular light water, but rather consists of 1 kton of pure heavy water (D_2O), contained in a 12 m diameter acrylic sphere. The heavy water target gives SNO three separate reactions for detecting solar neutrinos:

$$\begin{aligned} \nu_e + \mathrm{d} &\rightarrow \mathrm{p} + \mathrm{p} + \mathrm{e}^- \qquad \text{(CC)}, \\ \nu_x + \mathrm{d} &\rightarrow \mathrm{p} + \mathrm{n} + \nu_x \qquad \text{(NC)}, \\ \nu_x + \mathrm{e}^- &\rightarrow \nu_x + e^- \qquad \text{(ES)}. \end{aligned}$$

The charged current reaction (CC) is sensitive exclusively to electron-type neutrinos, while the neutral current reaction (NC) is equally sensitive to all active

neutrino flavors ($x = e, \mu, \tau$). The elastic scattering reaction (ES) is sensitive to all flavors as well, but with reduced sensitivity to ν_μ and ν_τ. Measuring the rates of all three reactions allows SNO to determine the flavor content of the ^{8}B neutrino flux.

In the initial phase of the SNO experiment (Nov 1999 - May 2001), SNO detected neutrons produced by NC interactions by observing the reaction $n + d \rightarrow t + \gamma$. The resulting γ-ray, with an energy of 6.25 MeV, Compton scatters to produce a relativistic electron that produces a ring of Cherenkov radiation. This phase of the experiment, in which neutrons were observed by their capture on deuterium, is known as SNO's "pure D_2O phase", since the center of the detector contained only pure heavy water.

2.1 Integral flux results

The astute reader will notice that if one detects neutrons by the single gamma-ray produced by neutron capture on a deuteron, then the CC, ES, and NC signals each consist of a single relativistic electron. Obviously there is no way to identify the neutrino reaction that produced the electron on an event-by-event basis. Fortunately, the three neutrino signals can be statistically separated. Each signal produces characteristic distributions for the electron's energy, radial position in the detector, and direction with respect to the Sun, as shown in Figure 4. For example, the CC reaction with ^{8}B neutrinos produces a known electron spectrum, a radial distribution that is uniform inside the heavy water and zero in the light water, and an angular distribution that is mildly anticorrelated with the Sun's direction. ES events show a strong directional peak pointing away from the Sun. Neutron captures of NC events produce a peak around an electron kinetic energy of 5 MeV, a radial distribution that peaks in the center of the detector, and an isotropic angular distribution. By fitting these probability distribution sets to SNO's data set, one can infer the rate of each reaction, and determine the "flux" from each reaction time.

Although this process, known as "signal extraction", uses energy, radial, and angular information to distinguish between different types of events, in practice the energy spectrum provides most of the constraint separating the numerically dominant CC and NC events. (The ES rate is $\sim 10\times$ smaller than the CC rate.) Figure 5 shows the energy spectrum of candidate neutrino events, after an kinetic

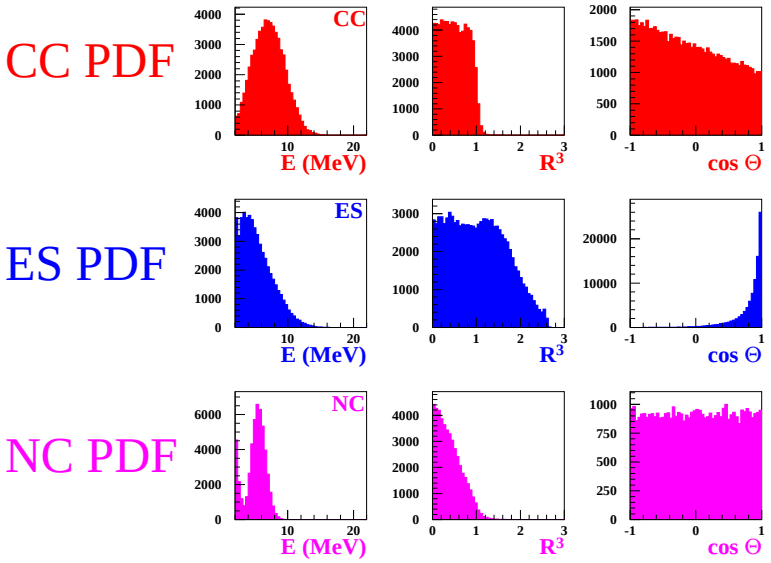

Figure 4: Signal PDFs for the CC, ES, and NC signals in pure D_2O. The three columns show the total electron energies, their radial locations in the detector ($R^3 = (r/600\text{ cm})^3$, with the edge of the heavy water at $R^3 = 1$), and angular distribution with respect to the Sun.

energy threshold of $T > 5$ MeV and a fiducial volume cut of $R < 550$ cm have been applied to reduce backgrounds from low energy radioactivity.[12] The neutrons show up as a peak sitting on top of the CC energy spectrum.

This means of identifying neutrons from NC interactions implicitly assumes that the CC and ES energy spectra follow their standard, undistorted shapes. This corresponds to the assumption of an energy-independent oscillation probability. This assumption is sufficient for testing the "null hypothesis" that neutrinos do not oscillate. Of course if solar neutrinos do oscillate, then an energy dependence in the oscillation probability is expected. In that case, derived fluxes from the analysis may be different from the true fluxes because of spectral distortions, but one can still test the hypothesis of no oscillations. (It turns out that for the favored Large Mixing Angle region of mixing parameters, the variation of the oscillation probability in SNO's energy region is small, and the assumption of an undistorted energy spectrum is not far from reality.)

Figure 6 shows the neutrino "fluxes" produced from SNO's pure D_2O data set using this fit procedure, relative to the SSM predicted values. Normalized to the

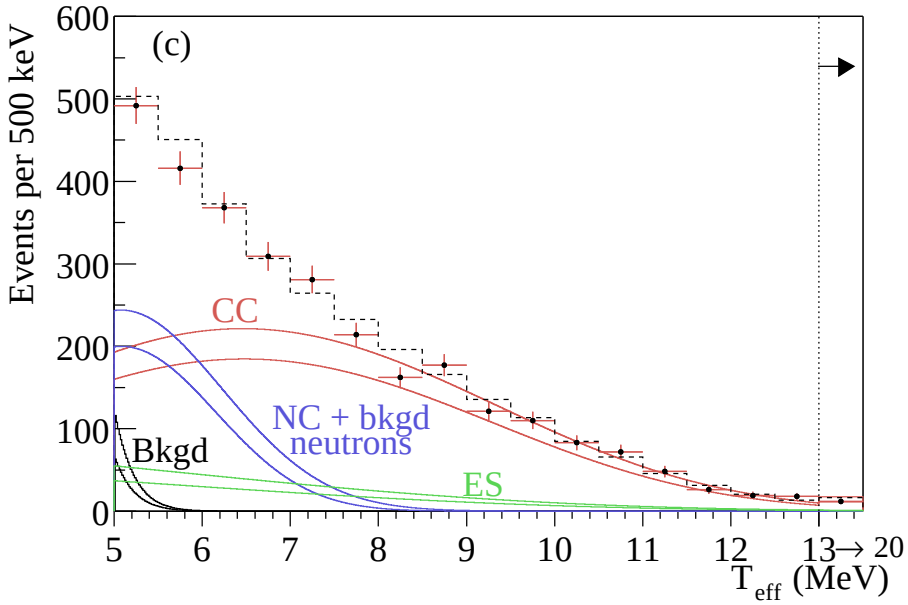

Figure 5: Energy spectrum of candidate neutrino events for the D_2O data set. The colored bands show the electron energy spectra produced by CC, ES, and NC interactions (along with low energy background events), normalized by a fit to the data. The neutrons show up as a "peak" sitting on top of the CC energy spectrum.[12]

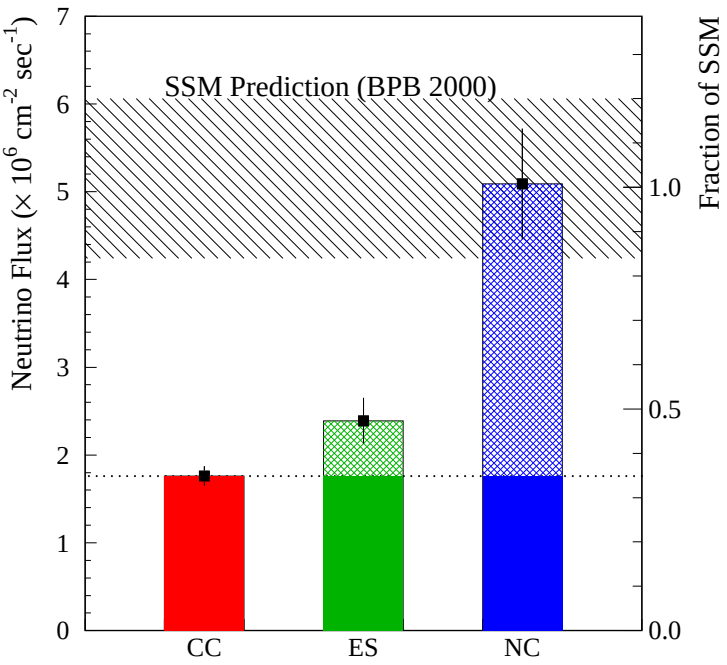

Figure 6: Ratio of the measured CC, ES, and NC reaction rates to the SSM predictions, assuming undistorted CC and ES energy spectra. The cross-hatched region corresponds to the solar model prediction.

integrated rates above the kinetic energy threshold of $T_{\rm eff} \geq 5$ MeV, the flux of ^{8}B neutrinos measured with each reaction in SNO, assuming the standard spectrum shape[13] is (all fluxes are presented in units of 10^6 cm^{-2}s^{-1})[12]:

$$\begin{aligned} \phi_{CC} &= 1.76^{+0.06}_{-0.05}(\text{stat.})^{+0.09}_{-0.09}\ (\text{syst.}) \\ \phi_{ES} &= 2.39^{+0.24}_{-0.23}(\text{stat.})^{+0.12}_{-0.12}\ (\text{syst.}) \\ \phi_{NC} &= 5.09^{+0.44}_{-0.43}(\text{stat.})^{+0.46}_{-0.43}\ (\text{syst.}) \end{aligned}$$

The null hypothesis of no neutrino oscillations with no spectral distortions predicts that the three reactions should all measure the same neutrino flux. The fact that the ES and especially NC reactions, which are sensitive to both electron and non-electron neutrino flavors, see a much higher rate than the CC reaction implies that there must be a non-electron component in the ^{8}B neutrino flux. The NC rate, which is equally sensitive to all active neutrino flavors, is in very good agreement with the SSM expectation, and is higher than the CC rate with $> 5\sigma$ statistical significance. These results strongly suggest that solar ν_e's do transform to other flavors, and that the total ^{8}B neutrino flux from the Sun is just what the SSM predictions say it should be.

2.2 Day-night asymmetry results

A day-night asymmetry in the neutrino flavor content would be independent evidence for neutrino oscillations, and the first direct evidence for matter effects modifying the oscillation probability. SNO has searched for day-night effects in its pure D_2O data set by dividing its data set into "night" and "day" portions, defined according to whether the Sun was below or above the horizon.[14] SNO's most unique contribution to solar neutrino physics is its sensitivity to different neutrino flavors, and so day-night asymmetries can be extracted for both the electron neutrino flux and the total active neutrino flux. The day-night asymmetry is usually presented as a ratio of the night and day fluxes as $A = 2(N-D)/(N+D)$, where N and D are the measured night and day fluxes.

There are actually two ways of treating the day-night asymmetry for the total active neutrino flux. Standard neutrino oscillation between active species predicts that this asymmetry should be zero, since oscillations should not change the total flux. So one can constrain $A_{total} = 0$ in the analysis. For a more model-independent result, we can relax the constraint, and fit for both the electron

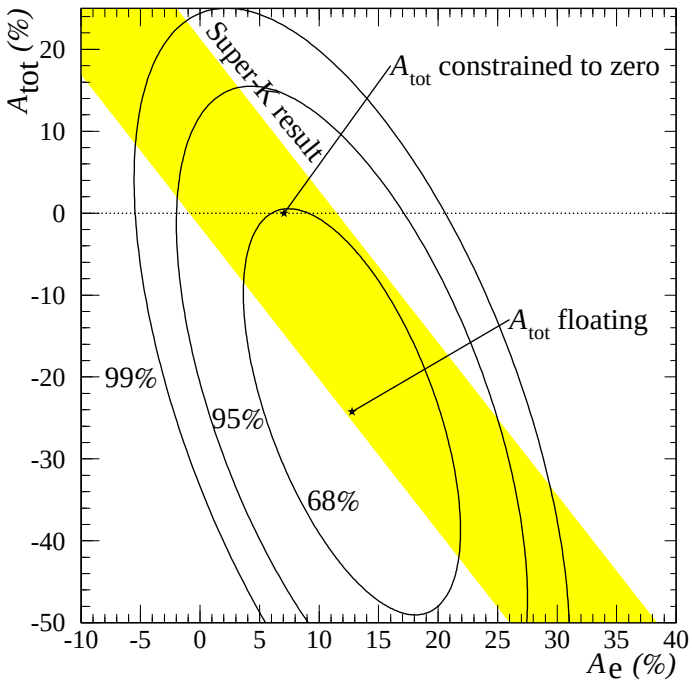

Figure 7: Joint probability contours for A_{tot} and A_e.[14] The points indicate the results when $\mathcal{A}_{\sqcup\wr\sqcup}$ is allowed to float and when it is constrained to zero. The diagonal band indicates the 68% joint contour for the Super-K A_{ES} measurement.

neutrino asymmetry A_e and the total flux asymmetry A_{total}.

Figure 7 shows contours for the extracted electron and total neutrino asymmetries.[14] Allowing A_{total} to float in the fit, the best-fit values are$A_e = 12.8 \pm 6.2^{+1.5}_{-1.4}\%$ and $A_{total} = -24.2 \pm 16.1^{+2.4}_{-2.5}\%$. If A_{total} is fixed to 0, then we get $A_e = 7.0 \pm 4.9^{+1.3}_{-1.2}\%$. All results were derived assuming an energy-independent survival probability.

SNO's day-night results are consistent with measurements of the day-night asymmetry of the ES rate by Super-Kamiokande.[9] The ES reaction has some sensitivity to both ν_e's and to other neutrino flavors, and so A_{ES} measures a linear combination of A_e and A_{total}. In Figure 7 the Super-K constraint is indicated by the diagonal yellow band, which overlaps to a large extent with SNO's day-night contours.

2.3 Constraints on mixing parameters

Figure 8 shows the allowed regions of MSW mixing parameters $(\Delta m^2, \tan^2\theta)$ from a two-flavor global solar neutrino analysis including the day and night total energy spectra from SNO's pure D_2O data set.[14] The so-called "Large Mixing Angle" (LMA) region, with $\Delta m^2 \approx 10^{-5} - 10^{-4}$ eV^2, is strongly favored over other solutions. This result was recently confirmed by the KamLAND experiment, which sees evidence for disappearance of reactor antineutrinos with mixing parameters in the LMA region.[15] Moreover, a maximal mixing angle ($\tan^2\theta_{12} = 1$) is ruled out at the $> 3\sigma$ level. The situation with the solar neutrino mixing angle contrasts with the case of atmospheric neutrinos, where maximal mixing ($\theta_{23} = \pi/4$) is favored.

3 Enhancing SNO's capacities with dissolved salt

Results from SNO's pure D_2O phase[16,12,14] have had a colossal impact on the field of solar neutrinos. In one fell swoop, these results established that neutrinos must change flavor, that SSM calculations of the ^{8}B neutrino flux were essentially correct, and that the Large Mixing Angle region of parameter space was strongly favored. However, the first SNO results have a number of limitations that should be emphasized as well:

- As noted previously, the analysis assumed that the CC and ES energy spectra

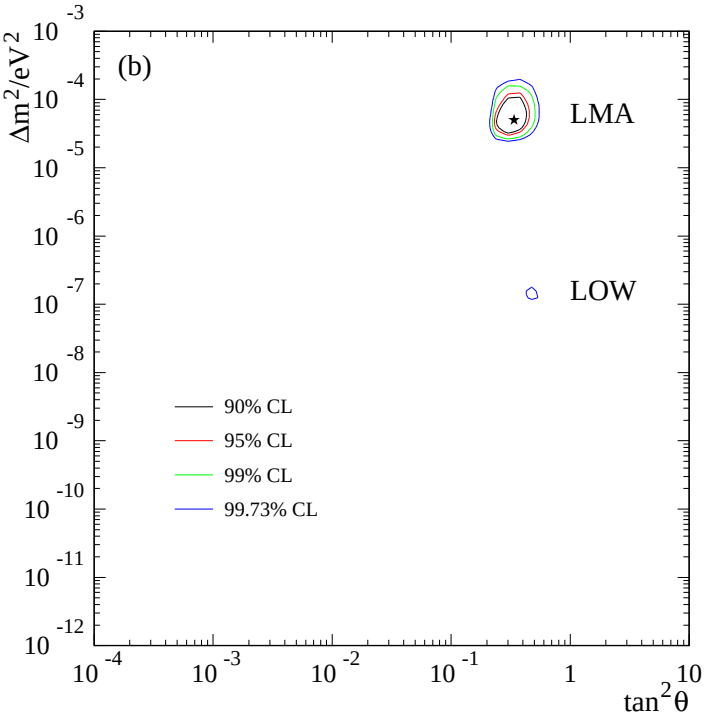

Figure 8: Allowed mixing parameters from a two-neutrino global analysis of solar neutrino data, including NC and day-night results from SNO's pure D_2O data set.[14] The Large Mixing Angle (LMA) solution is strongly favored over other solutions.

were undistorted. This assumption was appropriate for doing a null hypothesis test. Essentially the SNO results established that either solar neutrinos change flavor, or that there is a massive distortion in the shape of the CC and ES spectra that mimics an excess of NC events. Either way new neutrino physics is implied. However, the need to assume a spectral shape means that the derived fluxes are model-dependent. The effects of spectral distortions, which are expected at some level, will result corrections to the fluxes derived assuming no energy dependence in the neutrino oscillation probability.

- The statistical uncertainty on the NC flux weas relatively large, and much bigger than that on the CC flux.
- The signature of neutron capture on a deuteron is a single γ-ray of relatively low energy (6.25 MeV). This puts the peak of the NC signal at low energies relative to the CC signal, and close to the regime where low energy background radioactivity comes into play.
- SNO cannot distinguish $\nu_e \to \nu_\mu(\nu_\tau)$ oscillations from $\nu_e \to \bar{\nu}_\mu(\bar{\nu}_\tau)$. While the former process is theoretically favored, for solar neutrinos is not experimentally distinguishable from the latter. (Neither can one distinguish oscillations to ν_μ from oscillations to ν_τ. In the context of a 3-flavor oscillation analysis, solar neutrinos are actually expected to oscillate to a linear combination of ν_μ and ν_τ in about equal numbers.)

There is nothing to be done about the last point—this is a fundamental limitation of the physics itself. However, the other limitations can be partly overcome by making modifications to how SNO detects neutrons from NC interactions.

In June 2001 SNO attempted to do just this by dissolving sodium chloride into the heavy water to make a 0.2% solution. The addition of salt to the D_2O provides a new channel for detecting neutrons: namely, neutron capture on ^{35}Cl. Neutron capture of ^{35}Cl has a very high cross section, and the dissolved salt increases the detection efficiency for neutrons by about a factor of $\times 3$ more than the value for pure D_2O. Figure 9 shows the neutron capture efficiency vs. radius for pure D_2O and for salty brine as measured with a Cf neutron source.

Besides the large increase in statistics for NC events, chlorine captures have another significant advantage over looking for neutron captures on deuterons. Whereas the reaction $n + d \to t + \gamma$ produces a single γ-ray with an energy of 6.25 MeV, the reaction $n +^{35}$ Cl produces multiple γ's with a combined energy of

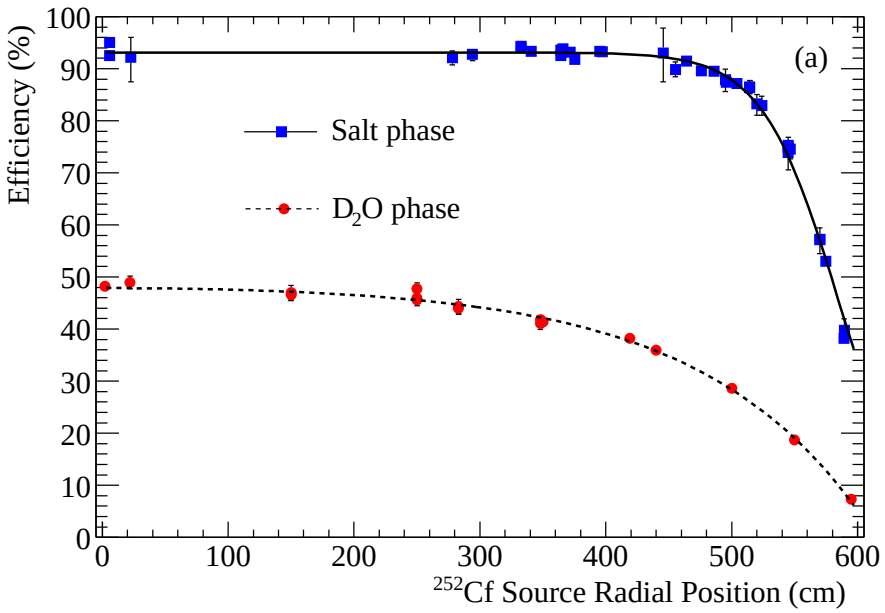

Figure 9: Neutron capture efficiencies on deuterons (pure D_2O) and on ^{35}Cl and deuterons (salt), for the two detector configurations, as a function of the radius at which the neutron is produced.[17]

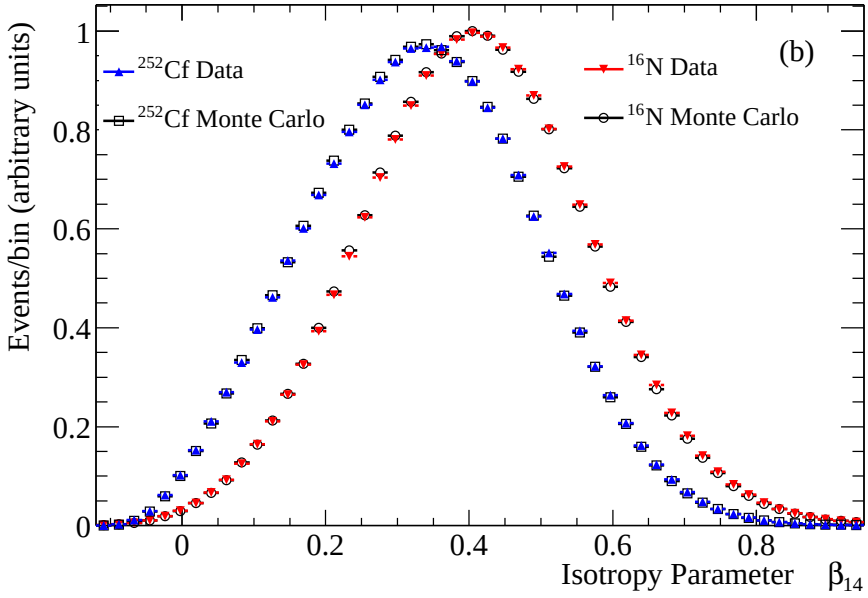

Figure 10: Distribution of the isotropy parameter β_{14} for ^{16}N (single electron) and ^{252}Cf (neutron capture) events. The distribution for neutron captures is shifted relative to the single electron distribution. Both distributions are modelled well by Monte Carlo.

8.6 MeV. Because multiple γ-rays are produced that can undergo Compton scattering, neutron capture events on chlorine produce a more isotropic light pattern on the phototube sphere than single-electron events, such as those produced by CC and ES interactions. An isotropy parameter can thus be defined for which NC events and CC/ES events will have different statistical distributions.

Event isotropy was characterized by parameters β_l, the average value of the Legendre polynomial P_l of the cosine of the angle between PMT hits. The combination $\beta_1 + 4\beta_4 \equiv \beta_{14}$ was selected as the measure of event isotropy to optimize the separation of NC and CC events. Figure 10 shows the distributions of β_{14} for single electron and neutron capture events, with a clear difference between the two.[17]

The isotropy parameter provides a new handle on separating CC/ES events from NC events. Now, instead of constructing three-dimensional signal PDFs in energy, radius, and angle, we can now construct 4-D PDFs using isotropy as the

fourth parameter. Figure 11 shows projections of the 4-D signal PDFs. While adding isotropy information improves the statistical separation of the neutrino signals, and thus lowers the statistical uncertainty, perhaps a more interesting scenario is to limit oneself to *three-dimensional* PDFs, replacing the energy variable by isotropy. The isotropy parameter thus allows a signal extraction that does not use energy, while still providing adequate separation between NC and CC/ES events. Such an extraction makes no assumption about the shapes of the CC and ES energy spectra, and so relaxes a significant model dependence in the analysis. (Strictly speaking, one does not want to remove energy completely from the problem, since the energy spectrum of NC events is well measured and has no model dependency. Instead, one can fit for the CC, ES, and NC fluxes in each energy bin, allowing the CC and ES fluxes in each bin to float freely while fixing the NC fluxes across bins to follow the expected energy spectra for NC events.)

In September 2003 the SNO collaboration released first results from its salt data set.[17] Integral CC, ES, and NC fluxes were extracted above a kinetic energy threshold of $T > 5.5$ MeV, making no assumptions about the energy dependence of the neutrino oscillation probability. The extracted flux values are (in units of 10^6 neutrinos per square centimeter per second):

$$\begin{aligned} CC &= 1.59 \ {}^{+0.08}_{-0.07}(\text{stat}) \ {}^{+0.06}_{-0.08}(\text{syst}) \\ ES &= 2.21 \ {}^{+0.31}_{-0.26}(\text{stat}) \ \pm 0.10 \ (\text{syst}) \\ NC &= 5.21 \ \pm 0.27 \ (\text{stat}) \ \pm 0.38 \ (\text{syst}) \end{aligned}$$

These fluxes agree well with those extracted from the D_2O data assuming no spectral distortions, and the NC flux agrees with the SSM prediction of 5.05×10^6.

Besides producing the first truly model-independent measure of the total flux of active neutrinos, SNO's salt results also significantly strengthen constraints on allowed mixing parameters. Figure 12 shows the allowed mixing parameters from an analysis that includes all solar neutrino results, including the new salt fluxes, and the reactor antineutrino results from KamLAND. A very small region of parameter space is selected. The CC and NC fluxes from the salt data especially constrain the mixing angle, which is shown to be smaller than maximal at 5.4σ significance.

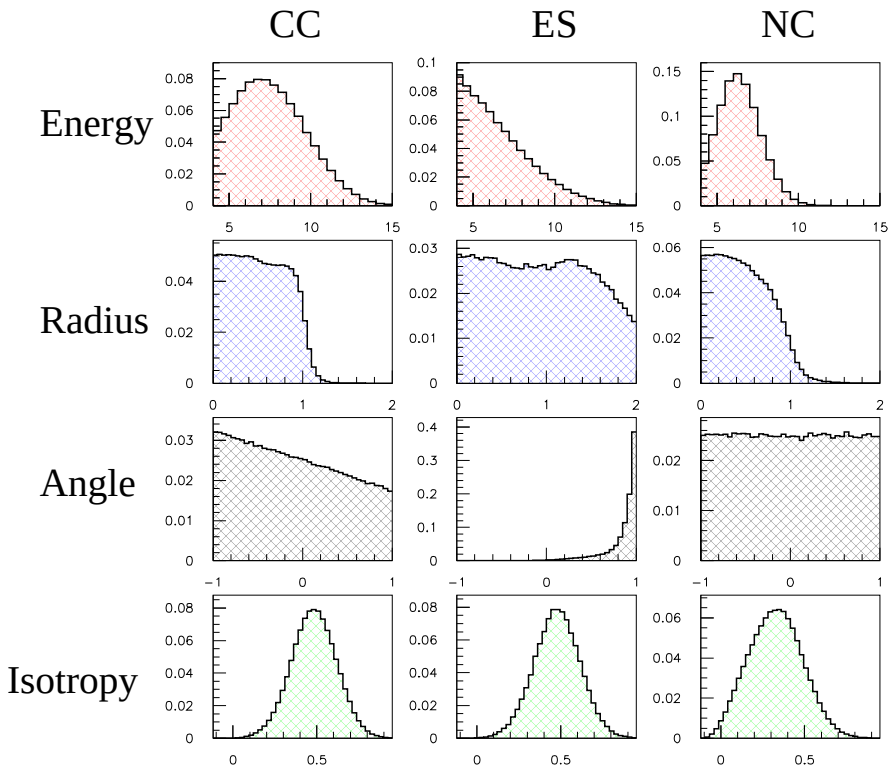

Figure 11: 1-D projections of the 4-dimensional salt PDFs for CC, ES, and NC events.

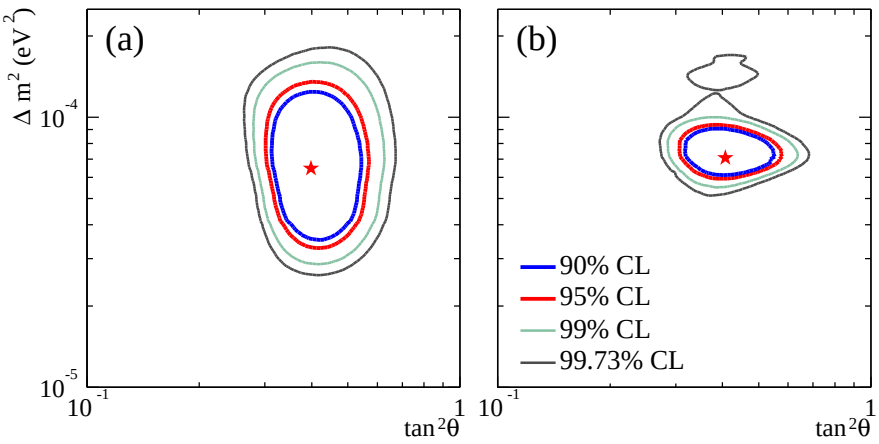

Figure 12: Allowed mixing parameters from a 2-flavor global analysis of solar neutrino and KamLAND results. Only the Large Mixing Angle solution is allowed, and maximal mixing is ruled out at 5.4σ.[17]

4 Anti-neutrino searches at SNO

While the SNO experiment was designed primarily to establish neutrino flavor transformations by measuring the CC and NC fluxes, it also has unique sensitivity to electron antineutrinos. Electron antineutrinos can interact in the SNO detector by:

$$\bar{\nu}_e + d \rightarrow e^+ + n + n \tag{3}$$

The energy threshold for this reaction is $E_\nu = 4.0$ MeV. This reaction results in a coincidence signature, in which a prompt positron can be detected, followed by the detection of one or both neutrons. The time interval between the positron detection and the neutron detection(s) is the neutron capture time, which is about 40 msec in pure heavy water.

There are three possible coincidence signatures, depending on which of the three particles are detected. The rarest is a triple coincidence, in which the positron and both neutrons are detected. The most common is a double coincidence between the positron and one of the neutrons. Finally, there is a "double neutron" signature, in which the positron falls below the analysis threshold, but both neutrons are over threshold. This last signature has a particularly low threshold, since seeing a positron above the analysis energy threshold is only possible

if the neutrino energy is at least 4.0 MeV greater than the analysis threshold, whereas the neutrons are visible even if the antineutrino is just above the reaction threshold, producing a sub-threshold positron. With an analysis threshold of $T > 5$ MeV, a fiducial volume cut of $R < 550$ cm, and a time coincidence window of 150 msec (chosen to be ≈ 3 times the mean neutron capture time), a preliminary estimate of the detection efficiencies for the three reactions using pure D_2O gives:

$$\begin{aligned}
\epsilon_{(e^+,n,n)} &= \ \ 1.11\,^{+0.05}_{-0.12}(\text{syst.}) \pm 0.02(\text{stat.})\,\% \\
\epsilon_{(e^+,n)} &= 10.27\,^{+0.37}_{-0.94}(\text{syst.}) \pm 0.05(\text{stat.})\,\% \\
\epsilon_{(n,n)} &= \ \ 1.20\,^{+0.05}_{-0.10}(\text{syst.}) \pm 0.02(\text{stat.})\,\%
\end{aligned}$$

This method of detecting individual antineutrino candidates with a coincidence signature has not previously been used by solar neutrino experiments. Super-Kamiokande has set limits on solar antineutrinos based upon the angular distribution of their event sample with respect to the Sun.[18] While ES interactions scatter electrons away from the Sun, producing a sharp angular peak, charged-current interactions of $\bar{\nu}_e$'s produce linear, negative slope in the angular distribution. By fitting the angular distribution of candidate events for ES, antineutrino, and background components, Super-Kamiokande has achieved limits on the $\bar{\nu}_e$ fraction in the solar neutrino flux. In contrast, SNO's double- or triple-coincidence signature allows antineutrino candidates to be identified on an event-by-event basis with a direct counting method.

Backgrounds to a $\bar{\nu}_e$ search include antineutrinos from known sources (e.g. atmospheric antineutrinos or neutrinos from nuclear reactors), and coincidence signatures produced by other sources. Examples of the latter include inelastic atmospheric ν interactions that produce multiple neutrons, and fission decays of ^{238}U. Other potential sources of coincidences include accidental (random) time coincidences between low energy events, multiple spallation neutrons produced by undetected muons, and various rare isotopic decays.

Electron antineutrinos are not produced by standard neutrino oscillations, and indeed $\nu_e \rightarrow \bar{\nu}_e$ oscillations would seemingly violate lepton number conservation. The SNO results suggest that solar ν_e's dominantly oscillate to ν_μ and ν_τ (or their antiparticles). The oscillations cannot be predominantly to $\bar{\nu}_e$, since their CC interactions in SNO would produce a very high neutron flux inconsistent with the

SNO data. The fact the KamLAND has observed the disappearance of reactor antineutrinos with mixing parameters consistent with the solar neutrino mixing parameters strongly suggests that neutrino flavor transformation of solar neutrinos is mostly due to standard MSW-enhanced neutrino oscillations. Nonetheless, it is still possible that other flavor transformation mechanisms could contribute at a subdominant level. These mechanisms could produce $\nu_e \to \bar{\nu}_e$ transitions. One such mechanism could be neutrino decay of a mass eigenstate, in which $\nu_2 \to \nu_1 + \nu_1 + \bar{\nu}_1$, with the $\bar{\nu}_1$ interacting as a $\bar{\nu}_e$.[19] Another mechanism capable of producing $\nu_e \to \bar{\nu}_e$ transitions is spin flavor precession (SFP).[20,21] The SFP mechanism supposes that neutrinos have a small magnetic moment, on the order of $10^{-11} - 10^{-10}\mu_B$. If in addition neutrinos are Majorana particles (so that the neutrino is its own antiparticle, but with opposite helicity), then the ν's magnetic moment can couple to the strong magnetic fields in the Sun, flipping the spin of the neutrino while simultaneously causing it to change flavors. The SFP effect thus can produce $\nu_e \to \bar{\nu}_\mu$ transitions. Standard neutrino oscillations can then go on to produce $\bar{\nu}_\mu \to \bar{\nu}_e$ transitions. Thus a combination of spin flavor precession and MSW-enhanced oscillations could work together to convert some small fraction of the solar neutrino flux to $\bar{\nu}_e$'s. Observation of spin flavor precession would be a monumental discovery, simultaneously proving that neutrinos are Majorana particles while showing that total lepton number can be violated. (Nonetheless, assuming that $\bar{\nu}_e$'s coming from the Sun were observed, it would still be necessary to demonstrate that spin flavor precession was the cause, and not some other mechanism such as neutrino decay.)

The SNO collaboration is in the final stages of preparing a publication limiting the solar $\bar{\nu}_e$ flux, and the reader is referred to that publication for results and details of the analysis.[22]

5 Conclusions

After its slow beginnings over 35 years ago, the field of solar neutrino research has made extremely rapid progress in just the last three years. Results from the Sudbury Neutrino Observatory have definitively established that solar neutrinos do convert to non-electron flavors. Global analyses of data from SNO, other solar neutrino experiments, and KamLAND place tight constraints on allowed neutrino mixing parameters. Measurements of the solar neutrino mixing angle θ_{12} are

particularly interesting in that while the mixing angle is large (as is the case for atmospheric neutrinos but unlike quarks), maximal mixing is now ruled out at greater than 5σ significance (whereas atmospheric neutrino results consistently favor maximal mixing for θ_{23}). While the data strongly support MSW-enhanced neutrino oscillations as the solution to the "solar neutrino problem" (now an outdated term), increasingly precise measurements are needed to quantitatively test this paradigm, and to look for deviations that could hint at further surprises (e.g. sterile neutrinos, spin flavor precession, etc.) With any luck, the elusive neutrino will continue to delight and surprise for years to come.

6 Acknowledgements

This research was supported by: Canada: NSERC, Industry Canada, NRC, Northern Ontario Heritage Fund Corporation, Inco, AECL, Ontario Power Generation; US: Dept. of Energy; UK: PPARC. We thank the SNO technical staff for their strong contributions. In the time between the 2003 SLAC Summer Institute and the submission of these proceedings, the author relocated from the University of Pennsylvania to the University of British Columbia, and thanks both institutions for their generous support.

References

[1] John N. Bahcall, M.H. Pinsonneault, and Sarbani Basu, Astrophys J. **555**, 990 (2001).

[2] B. T. Cleveland et al., Astrophys. J **496**, 505 (1998).

[3] J. N. Abdurashitov et al., Phys. Rev. C **60**, 055801 (1999).

[4] J. N. Abdurashitov et al. (2002), astro-ph/0204245

[5] M. Altmann et al., Phys. Lett. B **490**, 16 (2000).

[6] W. Hampel *et al*, Phys. Lett. B **447**, 127 (1999).

[7] C. M. Cattadori *et al.*, in *Proceedings of the TAUP 2001 Workshop*, (September 2001), Assergi, Italy.

[8] S. Fukuda *et al.*, Phys. Rev. Lett. **86**, 5651 (2001).

[9] S. Fukuda *et al.*, Phys. Lett. B **539**, 179 (2002).

[10] S. P. Mikheyev and A. Y. Smirnov, in *'86 Massive Neutrinos in Astrophysics and in Particle Physics, Proceedings of the Moriond Workshop*, edited by O. Fackler and J. Tran Thanh Van (1986), vol. Editions Frontières, Gif-sur-Yvette, 1986, p. 335.

[11] The SNO collaboration, *Nucl. Instr. and Meth.* **A449**, 172 (2000).

[12] Q.R. Ahmad *et al.*, *Phys. Rev. Lett.* **89**, 011301 (2002).

[13] C. E. Ortiz *et al.*, *Phys. Rev. Lett.* **85**, 2909 (2000).

[14] Q.R. Ahmad *et al.*, *Phys. Rev. Lett.* **89**, 011302 (2002).

[15] K. Eguchi *et al.*, Phys. Rev. Lett. **90**, 021802 (2003).

[16] Q.R. Ahmad *et al. Phys. Rev. Lett.* **87**, 071301 (2001).

[17] S.N. Ahmed *et al.*, submitted to *Phy. Rev. Lett.*, hep-ex/0309004, 2003.

[18] Y. Gando *et al.*, Phys. Rev. Lett. **90**, 171302 (2003).

[19] John F. Beacom and Nicole F. Bell, Phys. Rev. D **65**, 113009 (2002).

[20] O.G. Miranda *et al.*, *Nucl. Phys. B* 595, 360 (2001); B.C. Chauhan, J. Pulido, *Phys. Rev. D*66, 053006 (2002)

[21] E.Kh. Akhmedov, J. Pulido, *Phys. Lett. B* 553, 7(2003)

[22] Q.R. Ahmad *et al.*, manuscript in preparation.